nature nanotechnology

LETTERS

PUBLISHED ONLINE: 8 DECEMBER 2013 | DOI: 10.1038/NNANO.2013.255

# Molecular-sized fluorescent nanodiamonds

Igor I. Vlasov[1], Andrey A. Shiryaev[2], Torsten Rendler[3], Steffen Steinert[3], Sang-Yun Lee[3], Denis Antonov[3], Márton Vörös[4], Fedor Jelezko[5], Anatolii V. Fisenko[6], Lubov F. Semjonova[6], Johannes Biskupek[7], Ute Kaiser[7], Oleg I. Lebedev[8], Ilmo Sildos[9], Philip. R. Hemmer[10], Vitaly I. Konov[1], Adam Gali[4,11] and Jörg Wrachtrup[3]*

**Doping of carbon nanoparticles with impurity atoms is central to their application[1,2]. However, doping has proven elusive for very small carbon nanoparticles because of their limited availability and a lack of fundamental understanding of impurity stability in such nanostructures[3]. Here, we show that isolated diamond nanoparticles as small as 1.6 nm, comprising only ~400 carbon atoms, are capable of housing stable photoluminescent colour centres, namely the silicon vacancy (SiV)[4,5]. Surprisingly, fluorescence from SiVs is stable over time, and few or only single colour centres are found per nanocrystal. We also observe size-dependent SiV emission supported by quantum-chemical simulation of SiV energy levels in small nanodiamonds. Our work opens the way to investigating the physics and chemistry of molecular-sized cubic carbon clusters and promises the application of ultrasmall non-perturbative fluorescent nanoparticles as markers in microscopy and sensing.**

Nanometre-sized fluorescent emitters are needed as probes for fluorescence imaging with minimal perturbation in applications ranging from materials science to probing protein interactions in living cells[6]. Dye molecules have a very high brightness per unit volume or mass, but are usually not photostable at room temperature. To overcome this limitation, quantum dots were developed[7,8]. Semiconductor quantum dots can have a core size of a few nanometres; however, their total size increases up to ~10 nm when an outer passivation layer is added. Fluorescing centres in diamond are very attractive in this respect because of the rigidity of the diamond lattice and its wide bandgap, which cause a localization of 'optical' electrons within one to two interatomic distances from the defect. However, doping of nanodiamonds is perceived to have a size limit, depending on the defect centre. As an example, calculations have predicted nitrogen to be thermodynamically unstable in nanodiamonds with less than 2 nm in sizes[3]. In contrast, silicon-vacancy (SiV) defects in hydrogen-passivated truncated octahedral nanodiamonds have been predicted theoretically to be stable in particles of ~2 nm in diameter[9]. In accordance with this work our simulation indicates that the SiV centres are thermodynamically stable even in nanodiamonds with sizes ranging from 1.1 nm to 1.8 nm. At these sizes, *ab initio* calculations (see below) do show a quantum confinement effect in nanodiamonds[10,11], leading to an increase in the optical gap and changing the fluorescence photon energy of defects. Because the smallest man-made fluorescent isolated nanodiamonds to date have sizes limited to ~5 nm (refs 12,13), observation of this phenomenon has remained elusive. However, it is known that some types of meteorite contain nanodiamonds, presumably of presolar origin[14]. Their sizes range from 1 nm to 10 nm (refs 14,15) and, recently, SiV fluorescence has been found in this material[16]. In the present work we use such nanodiamonds with sizes less than 2 nm for investigation of the fluorescence properties of the SiV centres.

Initially our experimental work was motivated by calculations that suggest the stability of the SiV defect centre in nanodiamonds smaller than 2 nm. Owing to the small size of our nanoparticles, we modelled them using quantum-mechanical calculations in the largest quantum confinement limit; that is, the surface was fully terminated with hydrogen atoms. We calculated formation energies for the SiV defect in 1.1–1.8 nm nanoparticles by first-principles density functional theory (DFT). A SiV defect was modelled with a silicon atom located between two vacant sites of diamond lattice[17] (Fig. 1). For small nanodiamonds, the formation energy,

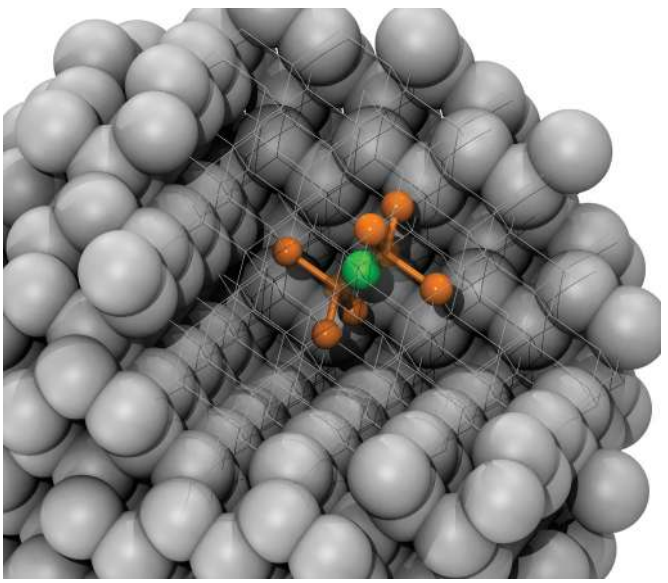

**Figure 1 | Structure of SiV centre in diamond.** Schematic representation of a small nanodiamond with an embedded SiV.

[1]General Physics Institute RAS, Vavilov Street 38, 119991 Moscow, Russia, [2]Institute of Physical Chemistry and Electrochemistry RAS, Leninsky pr. 31, 119071, Moscow, Russia, [3]3rd Physical Institute and Research Center SCOPE, University of Stuttgart, Pfaffenwaldring 57, 70550 Stuttgart, Germany, [4]Department of Atomic Physics, Budapest University of Technology and Economics, Budapest, Budafoki út 8, H-1111, Hungary, [5]Institute for Quantum Optics, University of Ulm, Albert-Einstein-Allee 11, 89081 Ulm, Germany, [6]Vernadsky Institute of Geochemistry and Analytical Chemistry RAS, Kosygin Street 19, Moscow, Russia, [7]Central Facility of Electron Microscopy, University of Ulm, Albert-Einstein-Allee 11, 89081 Ulm, Germany, [8]Laboratoire CRISMAT, UMR 6508 CNRS ENSICAEN, 6 boulevard Marechal Juin, 14050 Caen, France, [9]Institute of Physics, University of Tartu, Riia Street 142, 51014 Tartu, Estonia, [10]Department of Electrical and Computer Engineering, 3128 Texas A&M University, College Station, Texas 77843-3128, USA, [11]Institute for Solid State Physics and Optics, Wigner Research Centre for Physics, Hungarian Academy of Sciences, PO Box 49, 1525 Budapest, Hungary. *e-mail: wrachtrup@physik.uni-stuttgart.de

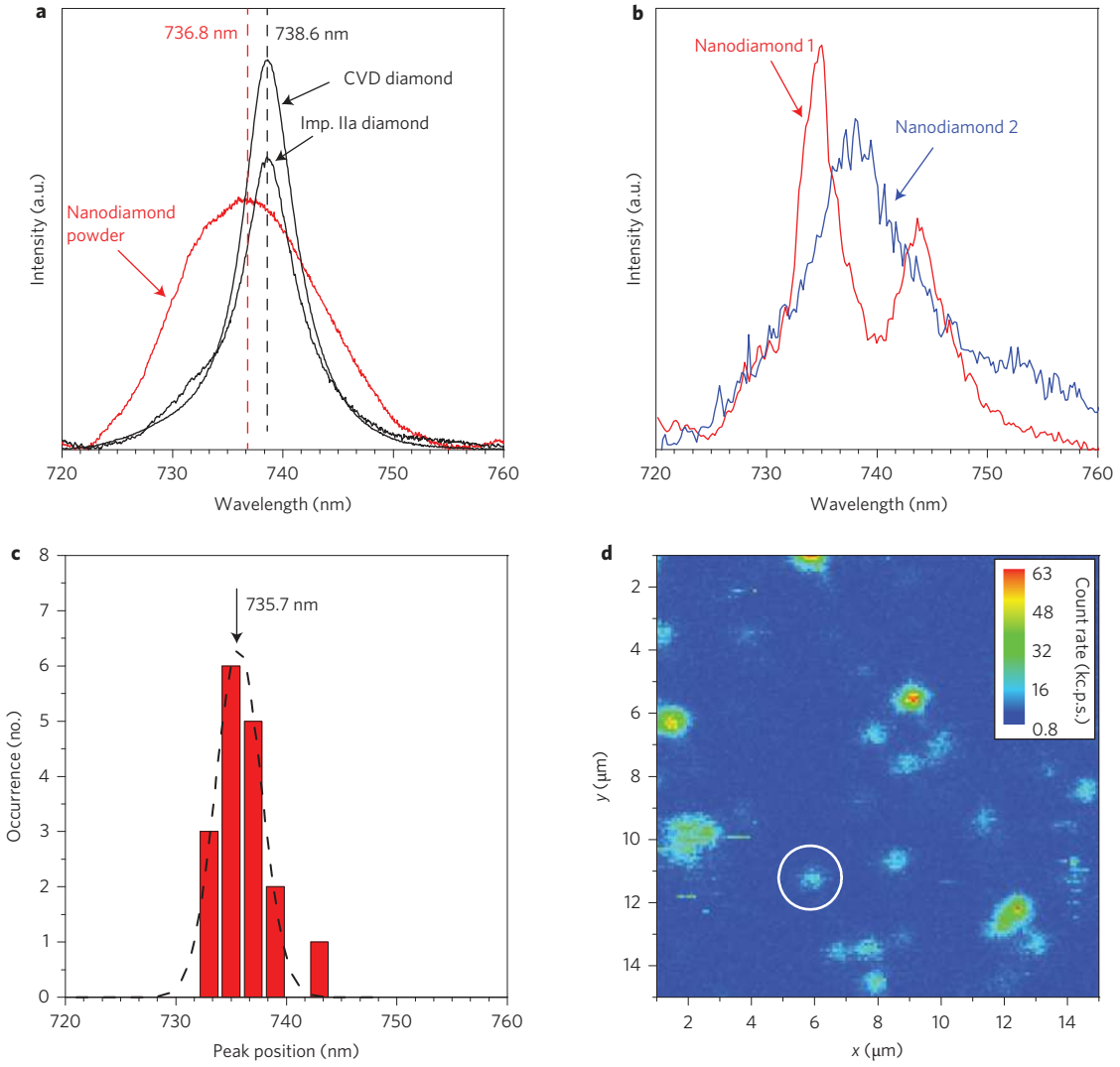


**Figure 2 | Photoluminescence analysis of the meteoric nanodiamonds. a**, Background-subtracted SiV photoluminescence spectra measured with 488 nm laser excitation at room temperature for meteoritic nanodiamond powder, CVD diamond single crystal and $Si^+$-implanted type IIa (Imp. IIa) diamond. The position of the SiV peak maximum is 736.8 nm for the meteoric nanodiamond powder, and 738.6 nm for CVD and natural diamonds. **b**, Photoluminescence spectra of two exemplary nanodiamonds dispersed on a silica slide. Nanodiamond 1 is marked in the confocal scan image (**d**) by a white circle and its photon statistics are also analysed in Fig. 5. **c**, Peak positions of all analysed spectra. The average of all peak maxima is 735.7 nm. **d**, Confocal fluorescence scan image of the dispersed nanodiamond sample using a red laser and 9 mW excitation power.

characterizing the stability of the defect structure, may critically depend on the placement of defects. However, for the SiV, our findings are that the formation energies are identical, within 0.1 eV, for every nanodiamond size when the defects are placed in the centre of the particle (see Supplementary Fig. 3). This suggests that there is no 'self-purification'[18] effect for SiV defects; that is, they remain stable even in very small nanodiamonds. Also, when the defect is placed near the surface (with only a single carbon atom separating the core of the defect from the surface), the formation energy is ~0.2 eV smaller for a negatively charged SiV than their corresponding value in the centre of the grain. With such a small energy difference there is no significant driving force acting to cause the defect to diffuse out to the surface, thereby resulting in stable SiVs even in very small nanodiamonds.

Excitation-state energies were determined using time-dependent density functional theory (TD-DFT), taking into account nuclear motion due to excitation. Because of quantum confinement (see also refs 19 and 20), a fully occupied and a partially occupied *e* state (see below) appear in the gap of our nanodiamonds. These *e* states are strongly localized on the carbon dangling bonds of the SiV defect. The lowest-energy excitation occurs predominantly between these fully occupied and partially occupied *e* defect states. The energy and the forces in the excited state were determined using TD-DFT. The calculated zero-phonon line (ZPL) energies of the negatively charged SiV defects are between 1.85 eV and 1.75 eV in 1.1 nm to 1.8 nm nanodiamonds. We observe a quantum confinement effect on the bandgap of nanodiamonds similar to that previously observed experimentally, whereby the valence band maximum of the nanodiamonds is lowered (with decreasing particle size) with respect to the vacuum level. This considerably downshifts the position of the fully occupied *e* defect level via exchange and correlation interactions between this *e* state and the host diamond states (Supplementary Fig. 5). As a consequence, there is a trend of increased energies for the lowest electronic transition of the SiV with decreasing particle size. Indeed, in our experimental data (discussed below) we observe such a trend in 1.6 nm nanodiamonds.

To test our theoretical predictions, meteoritic nanodiamonds were extracted from the Efremovka CV3 chondrite[21]. Defect luminescence was characterized by a narrow ZPL near 738 nm (1.68 eV) in the photoluminescence spectrum[16,22]. Figure 2a

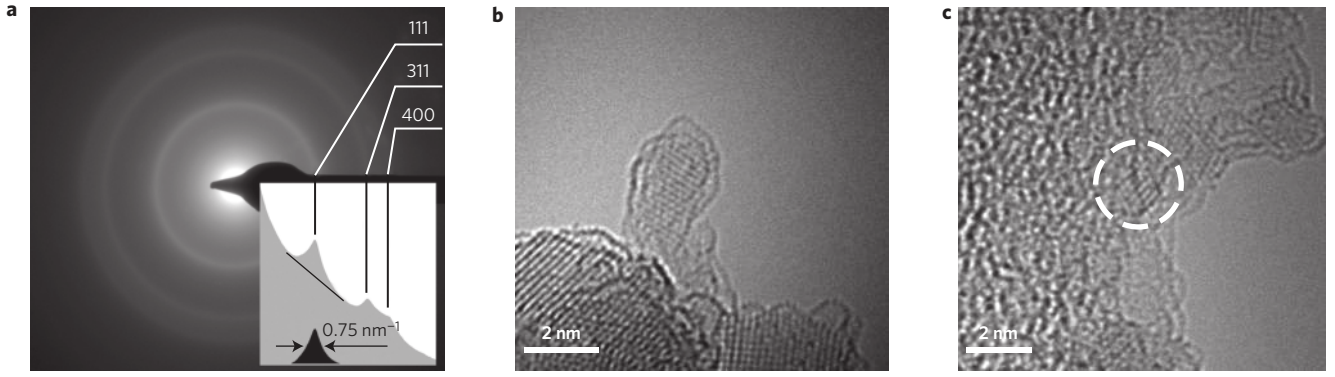


**Figure 3 | HRTEM analysis of meteoritic nanodiamonds. a**, The electron diffraction ring pattern is evidence for the diamond crystal structure. Inset: intensity plot profile and background subtracted peak intensity of the 111 ring. **b**, AC-HRTEM image of free-standing nanodiamond grain (size, 2 nm). **c**, AC-HRTEM image of nanodiamond grain (size, 1 nm) (encircled).

shows the SiV fluorescence emission spectra measured for two bulk diamond samples (silicon-doped chemical vapour-deposited (CVD) diamond single crystal and a natural type IIa diamond implanted with silicon ions) in comparison with a representative SiV spectrum of nanodiamond powder containing a large number of fluorescent particles. As can be seen in Fig. 2a, there is a blueshift of 0.004 eV of the SiV peak from meteoritic nanodiamonds ensembles relative to that of SiV in bulk diamonds. For further analysis, nanodiamonds from colloidal solution were dispersed on a silica slide and analysed by confocal microscopy. Fluorescence of most spots was stable for at least 5 min, which is sufficient to acquire high-quality photoluminescence spectra. Some spots do show long-time-stable (>24 h) photoluminescence from single nanodiamonds (see below). The photoluminescence spectra of two nanodiamonds are shown in Fig. 2b. Nanodiamonds typically show one or two resolved emission peaks, with significant shifts between the spectra from different nanoparticles. Variations in the SiV emission band position (Fig. 2b,c) can be explained by the existence of strong lattice stress in diamond nanoparticles, similar to that in CVD nanodiamonds[23] where at low temperature this is accompanied by a redshift of emission[24], or probably isotopic enrichment of silicon ($\Delta E = 1$ meV; ref. 16) in some particles due to their extraterrestrial source. This finding also explains the widely broadened emission peak of the nanodiamond powder (Fig. 2a). The main peak positions of all analysed fluorescent nanodiamonds are shown in Fig. 2c. The average position of all peaks (735.7 nm) is shifted to higher energies by 0.007 eV, which is close to the shift of 0.004 eV from nanodiamond powder.

To obtain more information about the spatial dimensions of the diamond nanoparticles, they were analysed by aberration-corrected high-resolution transmission electron microscopy (AC-HRTEM). Selective area electron diffraction (SAED) analysis revealed that the investigated fraction of diamond grains in the analysed sample have a characteristic size below 2 nm. This characteristic size was determined from the half-width of the 111 diffraction peak of the SAED patterns with a value of 0.75 nm$^{-1}$. This corresponds to a crystallite size of 1.3 nm, as shown in Fig. 3a. The smallest free-standing diamond grain found in the sample was 2 nm in size (Fig. 3b). Nanodiamond crystallites with size down to 1 nm were observed in small agglomerates (Fig. 3c). To further explore nanodiamond size without the need for immobilization on a support structure and hence aggregation, nanodiamond solutions were investigated using fluorescence correlation spectroscopy (FCS)[25]. FCS provides a highly sensitive quantitative statistical analysis of fluorescence fluctuations, which can be used to determine the hydrodynamic radius of fluorescent diamond nanoparticles containing SiV centres[26]. The size of the particles was derived from the characteristic diffusion time of the particles through the confocal volume. Figure 4 presents a comparison of two autocorrelation functions determined for nanodiamonds and Rhodamine 6G dye molecules under identical experimental conditions. From the autocorrelation function the mean fluorescent nanodiamond particle size was estimated to be $1.6 \pm 0.2$ nm.

To evaluate the photon statistics of the SiV fluorescence, nanodiamonds immobilized on a fused-silica slide were investigated. An autocorrelation function $g^{(2)}$ was measured for one of the fluorescent nanodiamond spots (Fig. 5a) (see also the spectrum of nanodiamond 1 in Fig. 2b). Fitting the background-corrected autocorrelation function and assuming emission of multiple identical emitters[4,27] revealed three emitters within the fluorescent spot. The fitting routine also took into account the set-up-related jitter by deconvoluting the measured autocorrelation function with a Gaussian response function. To further characterize the emitters, its saturation intensity was measured to be 38 kc.p.s. (kilocounts per second; Fig. 5b) resulting in 12.7 kc.p.s. per emitter. These rates are comparable to single SiV centres produced by ion implantation in bulk diamond[4], when taking into account the different

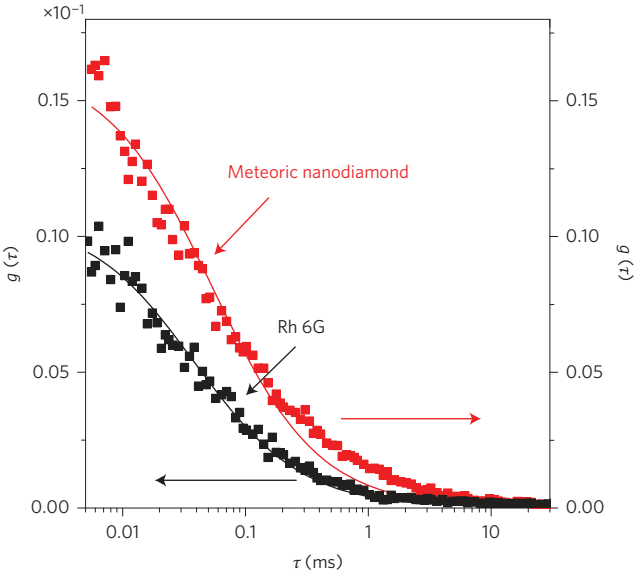


**Figure 4 | FCS measurement of luminescent meteoritic nanodiamonds and a dye molecule (Rhodamine 6G (Rh 6G)).** The fit (solid curve) of the measured autocorrelation function (red symbols) yields the characteristic diffusion time, resulting in an effective size of fluorescent particles of $1.6 \pm 0.2$ nm when using 0.6 nm as a reference for the hydrodynamic radius for Rhodamine 6G in water (calculated from refs 32 and 33) .

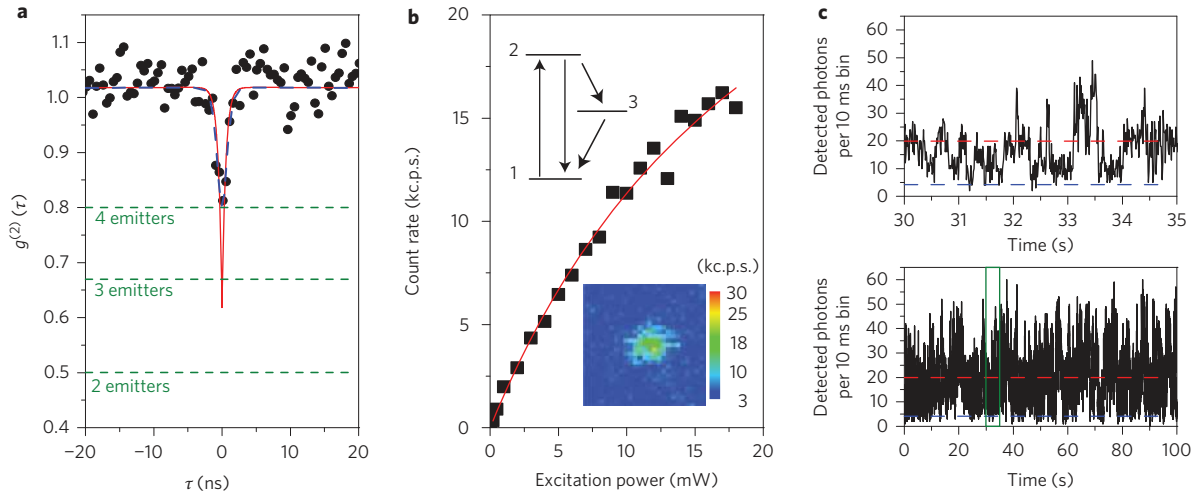


**Figure 5 | Detailed analysis of a fluorescent spot presumably containing only few emitters. a**, Autocorrelation function showing the background-corrected raw data (black) fitted with a model including the instrument response function (blue) and the found $g^{(2)}$ function (red) using the model from refs 4 and 27. The number of emitters within the analysed spot was found to be three. **b**, Saturation curve using 660 nm excitation. The fit (red) gives a saturation intensity of 38 kc.p.s. and a saturation power of 23 mW. Bottom inset: confocal image obtained using a fluorescent bandpass filter around SiV fluorescence at 9 mW. Top inset: the rate model showing the ground (1), excited (2) and metastable (3) states, and transitions between them used for the $g^{(2)}$ fit function. **c**, Time traces at 500 μW and 10 ms binning showing blinking of the analysed spot. The red line indicates the mean intensity over 100 s. The blue line shows the background level of the sample. In the upper graph the time traces are zoomed in for better visibility.

photon extraction efficiencies caused by the different sample geometries. Figure 5c presents fluorescence time traces with 10 ms binning, in time windows of 5 s and 100 s, respectively. The SiVs show blinking[5] but stably emit fluorescence over tens of minutes. Although the origin of this blinking is not clear as yet, it appears that it is related to the nanodiamond size rather than the SiV itself[5,12].

In conclusion we have demonstrated fluorescence emission from SiV defects in nanodiamonds with sizes below 2 nm. For the nanodiamonds, an average shift of 0.004 eV to higher emission energies, corresponding to an emission wavelength change of 1.8 nm, was found. Calculations indicate that this shift is due to a quantum confinement effect mediated by the valence band electrons of the nanodiamond. Our calculations also show that, similar to the ground states of most other defects in diamond, the SiV excited-state wavefunction is almost exclusively localized on the defect site. This, together with the fact that even the excited-state energy is ~2 eV below the conduction band of the nanocrystal, results in a high stability of the photoelectron on the defect site, and also leads to nanoparticles showing bulk and molecular properties with strongly modified bandgaps and surface-related absorption bands. Despite the apparent blinking of nanodiamonds, their emission is rather photostable and allows continuous long-time observation over tens of hours. These small nanodiamonds, with dimensions comparable to dye molecules, are therefore promising as, for example, fluorescent markers in cell biology where having sizes smaller than typical proteins is an important prerequisite. In addition, the SiV in diamond exhibits narrow-band near-infrared emission, another important criterion for life-science applications in terms of observable sample penetration depth and reduced autofluorescence[28]. Although the present work has used nanodiamonds from meteorites, current production technologies for nanodiamonds have achieved sizes of 2–5 nm (ref. 13). Our results provide substantial motivation to pursue further work on size reduction down to molecular sizes.

## Methods

The nanodiamond samples were extracted from the Efremovka CV3 chondrite using well-established processes involving multistage chemical treatment of the meteorite pieces by HF, HF + HCl, KOH, $H_2O_2$, $K_2Cr_2O_7$ and $HClO_4$ at various temperatures and isolation of the colloidal nanodiamond with high pH solution[21]. All samples had a translucent pale yellow colour, typical for the meteoritic colloidal diamond. Infrared absorption investigations[14] indicated that the main functional groups on the surface of the extracted meteoritic nanodiamond were oxygen-related groups: carboxyl, carbonyl and hydroxyl.

AC-HRTEM and electron diffraction experiments were performed on nanodiamond samples dispersed on a carbon grid using a FEI-TITAN 80-300 operated at 80 kV (to avoid knock-on damage) equipped with an image-side aberration corrector with a resolution of 0.15 nm and a JEOL 4000EX microscope operated at 400 kV and with 0.17 nm point resolution.

Photoluminescence spectra for the nanodiamond powder were recorded at room temperature using a LABRAM HR spectrometer with an $Ar^+$ laser for excitation. Laser radiation (power, 0.1 mW; wavelength, 488 nm) was focused on a spot (diameter, 2 μm) on the surface of the nanodiamond powder.

Fluorescence correlation spectroscopy was performed using a home-built confocal set-up with a high-numerical-aperture water objective (Olympus, UPlanApo ×60, NA 1.2). Samples dissolved in polyvinyl alcohol solution were excited using 0.1 mW of 532 nm laser radiation and their fluorescence was detected using an actively quenched avalanche photodiode. Fluorescence autocorrelation was recorded with a hardware correlator (ALV-5000).

To analyse the evaporated nanodiamond clusters on the fused-silica slide, an oil objective (Olympus, UPLSAPO 60XO, NA 1.35) was used. The SiV luminescence was filtered out by a bandpass filter (transmission 730–750 nm). For excitation, red laser diodes (emission peak wavelength, 660 nm and 690 nm; Thorlabs HL6548FG and HL6738MG) were used. The photoluminescence spectra were recorded using a broad bandpass filter (transmission 723–817 nm) and Czerny–Turner like spectrometer (Acton, SpectraPro300i, grating: 300 g $mm^{-1}$) combined with a back-illuminated liquid-nitrogen-cooled charge-coupled device camera (Princeton Instruments, LN/CCD-1340400 EHRB/I).

To determine the formation energy of the defects, we applied DFT calculations within a generalized gradient approximation Perdew-Burke-Ernzerhof (PBE). In bulk studies we used a 512-atom supercell and Γ-point for Brillouin-zone sampling in order to model the neutral and negatively charged SiV defect in diamond. In particular, we utilized the VASP code to determine the geometry of the defect, using the projector augmented wave method to eliminate the core electrons, while a plane-wave basis set was used to expand the valence wavefunctions. We applied the standard VASP projectors for the carbon, hydrogen and silicon atoms with a plane-wave cutoff of 420 eV. Geometry optimization was halted when the magnitude of the forces on the atoms was lower than 0.01 eV $Å^{-1}$.

The nanodiamonds were also studied with VASP code within the PBE functional, with the periodic images separated by vacuum of at least 1 nm, ensuring that the critical defect states (and any other occupied states) did not interact. Nanodiamonds were fabricated to form spherical shapes, which are in line with TEM experiments (Fig. 3b). The nanodiamonds had carbon atoms at the surface with two or fewer dangling bonds. The dangling bonds of the nanodiamonds were terminated by hydrogen atoms; this could correspond to the 'largest' quantum confinement limit because the C–H covalent bonds are stronger than any other (carbon, nitrogen or oxygen related) covalent bonds that may exist on their surface.

This idealistic model of nanodiamonds makes it possible to investigate the effect of quantum confinement, at its maximum limit, on the defect states when the defect is placed in nanodiamonds of different sizes. We also considered 2 × 1-like reconstructed nanodiamond surfaces on (100) facets. We found that the reconstruction has no effect on the electronic structure of SiV defects. More details and the corresponding references are provided in the Supplementary Information.

We found in bulk studies that the negatively charged defect is responsible for the 1.68 eV signal[29]. The calculated ZPL of the negatively charged defect is 1.72 eV, which agrees very well with the measured 1.68 eV in terms of the expected accuracy of *ab initio* methods[29]. We thus compared the calculated and measured photoluminescence lines for the negatively charged SiV defect.

To calculate the excitation energies we applied TD-DFT with the PBE0 hybrid density functional in the kernel by TURBOMOLE code. We utilized this methodology for tiny nanodiamonds where the experimental absorption spectra could be well reproduced as well as the vertical absorption energy of a nitrogen-vacancy centre[30]. The main interest here is the ZPL where the nuclei relaxes in the excited state, which lowers the ZPL energy with respect to the lowest vertical absorption energy. The energy and the forces in the excited state are determined at the TD-DFT level, as the complexity of the excited-state wavefunction requires more complex methods than usually used for constrained DFT approaches. We therefore calculated forces in the excited state within TD-DFT using PBE0 in the kernel, and obtained the minimum energy within the excited-state potential energy surface. (For further details see Supplementary Information.) The calculated Stokes shift of 0.12 eV in the SiV defect is in accordance with the experimental data extracted from absorption spectra of the 1.68 eV photoluminescence centre found in large nanodiamonds and bulk diamond[31].

Received 24 June 2013; accepted 28 October 2013; published online 8 December 2013

## References


1. Mochalin, V. N., Shenderova, O., Ho, D. & Gogotsi, Y. The properties and applications of nanodiamonds. *Nature Nanotech.* **7,** 11–23 (2012).
2. Hui, Y. Y., Cheng, C-L. & Chang, H-C. Nanodiamonds for optical bioimaging. *J. Phys.* **43,** 374021 (2010).
3. Barnard, A. S. & Sternberg, M. Substitutional nitrogen in nanodiamond and Bucky-diamond particles. *J. Phys. Chem. B* **109,** 17107–17112 (2005).
4. Wang, C., Kurtsiefer, C., Weinfurter, H. & Burchard, B. Single photon emission from SiV centres in diamond produced by ion implantation. *J. Phys. B* **39,** 37–41 (2006).
5. Neu, E., Agio, M. & Becher, C. Photophysics of single silicon vacancy centers in diamond: implications for single photon emission. *Opt. Express* **20,** 19956–19971 (2012).
6. Evanko, D. The new fluorescent probes on the block. *Nature Methods* **5,** 218–219 (2008).
7. Biju, V., Itoh, T., Anas, A., Sujith, A. & Ishikawa, M. Semiconductor quantum dots and metal nanoparticles: syntheses, optical properties, and biological applications. *Anal. Bioanal. Chem.* **391,** 2469–2495 (2008).
8. Taylor, A., Wilson, K. M., Murray, P., Fernig, D. G. & Lévy, R. Long-term tracking of cells using inorganic nanoparticles as contrast agents: are we there yet? *Chem. Soc. Rev.* **41,** 2707–2717 (2012).
9. Barnard, A. S., Vlasov, I. I. & Ralchenko, V. G. Predicting the distribution and stability of photoactive defect centers in nanodiamond biomarkers. *J. Mater. Chem.* **19,** 360–365 (2009).
10. Raty, J-Y., Galli, G., Bostedt, C., van Buuren, T. W. & Terminello, L. J. Quantum confinement and fullerenelike surface reconstructions in nanodiamonds. *Phys. Rev. Lett.* **90,** 037401 (2003).
11. Bolker, A., Saguy, C., Tordjman, M. & Kalish, R. Quantum confinement and Coulomb blockade in isolated nanodiamond crystallites. *Phys. Rev. B* **88,** 035442 (2013).
12. Bradac, C. *et al.* Observation and control of blinking nitrogen-vacancy centres in discrete nanodiamonds. *Nature Nanotech.* **5,** 345–349 (2010).
13. Vlasov, I. I. *et al.* Nanodiamond photoemitters based on strong narrow-band luminescence from silicon-vacancy defects. *Adv. Mater.* **21,** 808–812 (2009).
14. Lewis, R. S., Anders, E. & Draine, B. T. Properties, detectability and origin of interstellar diamonds in meteorites. *Nature* **339,** 117–121 (1989).
15. Daulton, T. L., Eisenhour, D. D., Bernatowicz, T. J., Lewis, R. S. & Buseck, P. R. Genesis of presolar diamonds: comparative high-resolution transmission electron microscopy study of meteoritic and terrestrial nano-diamonds. *Geochim. Cosmochim. Acta* **60,** 4853–4872 (1996).
16. Shiryaev, A. A. *et al.* Spectroscopic study of impurities and associated defects in nanodiamonds from Efremovka (CV3) and Orgueil (CI) meteorites. *Geochim. Cosmochim. Acta* **75,** 3155–3165 (2011).
17. Goss, J. P., Jones, R., Breuer, S. J., Briddon, P. R. & Öberg, S. The twelve-line 1.682 eV luminescence center in diamond and the vacancy-silicon complex. *Phys. Rev. Lett.* **77,** 3041–3044 (1996).
18. Erwin, S. C. *et al.* Doping semiconductor nanocrystals. *Nature* **436,** 91–94 (2005).
19. Chang, Y. K. *et al.* Quantum confinement effect in diamond nanocrystals studied by X-ray-absorption spectroscopy. *Phys. Rev. Lett.* **82,** 5377–5380 (1999).
20. Berg, T. *et al.* Quantum confinement observed in the X-ray absorption spectrum of size distributed meteoritic nanodiamonds. *J. Appl. Phys.* **104,** 064303 (2008).
21. Amari, S., Lewis, R. S. & Anders, E. Interstellar grains in meteorites: I. Isolation of SiC, graphite and diamond; size distributions of SiC and graphite. *Geochim. Cosmochim. Acta* **58,** 459–470 (1994).
22. Clark, C. D., Kanda, H., Kiflawi, I. & Sittas, G. Silicon defects in diamond. *Phys. Rev. B* **51,** 16681–16688 (1995).
23. Neu, E. *et al.* Single photon emission from silicon-vacancy colour centres in chemical vapour deposition nano-diamonds on iridium. *New J. Phys.* **13,** 025012 (2011).
24. Sternschulte, H., Thonke, K., Sauer, R., Münzinger, P. & Michler, P. 1.681-eV luminescence center in chemical-vapor-deposited homoepitaxial diamond films. *Phys. Rev. B* **50,** 14554–14560 (1994).
25. Krichevsky, O. & Bonnet, G. Fluorescence correlation spectroscopy: the technique and its applications. *Rep. Prog. Phys.* **65,** 251–297 (2002).
26. Neugart, F. *et al.* Dynamics of diamond nanoparticles in solution and cells. *Nano Lett.* **7,** 3588–3591 (2007).
27. Kitson, S. C., Jonsson, P., Rarity, J. G. & Tapster, P. R. Intensity fluctuation spectroscopy of small numbers of dye molecules in a microcavity. *Phys. Rev.* **58,** 620–627 (1998).
28. Neu, E. *et al.* Narrowband fluorescent nanodiamonds produced from chemical vapor deposition films. *Appl. Phys. Lett.* **98,** 243107 (2011).
29. Gali, A. & Maze, J. R. An *ab initio* study on split silicon-vacancy defect in diamond: electronic structure and related properties. Preprint at http://arXiv.org/pdf/1310.2137 (2013).
30. Gali, A. Time-dependent density functional study on the excitation spectrum of point defects in semiconductors. *Phys. Status Solidi B* **248,** 1337–1346 (2011).
31. Iakoubovskii, K., Adriaenssens, G. J., Dogadkin, N. N. & Shiryaev, A. A. Optical characterization of some irradiation-induced centers in diamond. *Diam. Relat. Mater.* **10,** 18–26 (2001).
32. Gendron, P-O., Avaltroni, F. & Wilkinson, K. J. Diffusion coefficients of several rhodamine derivatives as determined by pulsed field gradient–nuclear magnetic resonance and fluorescence correlation spectroscopy. *J. Fluoresc.* **18,** 1093–1101 (2008).
33. Müller, C. B. *et al.* Precise measurement of diffusion by multi-color dual-focus fluorescence correlation spectroscopy. *EPL Eur. Lett.* **83,** 46001 (2008).


## Acknowledgements

This work was supported in part by Russian Foundation for Basic Research (RFBR) grants nos 11-02-01432, 12-05-00208 and 12-03-00787, a grant from Russian Academy of Science (RAS) programme no. 24, a grant of the President of the Russian Federation for leading scientific schools (no. 3076.2012.2), an National Institutes of Health (NIH) grant (no. C09-00053), the European Commission, EU FP7 grants Diamond based atomic nanotechnologies (DIAMANT) and Development of diamond intracellular nanoprobes for oncogen transformation dynamics monitoring in living cells (DINAMO), as well as the European Research Council (ERC) (via project Spin Quantum Technologies (SQUTEC) Biology and Quantum (BioQ)), the Deutsche Forschungsgemeinschaft (DFG) (via Sonderforschungsbereiches (SFB) 716) and the Volkswagenstiftung.

## Author contributions

I.V., J.W., P.H. and F.J. designed and coordinated the experiment. I.V., A.A.S., L.F.S., A.V.F., O.I.L., V.I.K. and I.S. prepared and characterized the sample. U.K. and J.B. carried out the high-resolution electron microscopy. T.R., S.S. and S.Y.L. designed, set up and carried out fluorescence measurements. A.G., D.A. and M.V. carried out the calculations and analysed the simulation data. I.V., T.R., S.Y.L., A.G., P.H. and J.W. wrote the manuscript.

## Additional information

Supplementary information is available in the online version of the paper. Reprints and permissions information is available online at www.nature.com/reprints. Correspondence and requests for materials should be addressed to J.W.

## Competing financial interests

The authors declare no competing financial interests.